Available online at www.sciencedirect.com

ScienceDirect

Procedia Engineering 14 (2011) 743–752

Procedia Engineering

www.elsevier.com/locate/procedia

The Twelfth East Asia-Pacific Conference on Structural Engineering and Construction

Investigation of RBS Connection Ductility in Eccentrically Braced Frame

M. Naghipour[1*], N. Javadi[2†], A. Naghipour[3]

[1]*Department of Civil Engineering, Babol University of Technology, Iran*
[2]*Department of Engineering, University of Shomal, Iran*
[3]*Department of Civil Engineering, University of Manchester, UK*

Abstract

In the eccentrically braced frames (EBF) in which one end of the link is connected to a column, the integrity of the link-to-column connection is essential to the ductile performance and safety of the EBF. But among of all tests that have taken place on this connection, because of the intensity of stresses on the link to column connections, the tested specimens were confronted with brittle and sudden failures. So it seems that the reduced beam sections (RBS), in flexural yielding links can be a suitable solution for raising this problem by concentrating stresses at a location away from the connection. Therefore in this paper, by using a finite element program ETABS and with nonlinear static analysis (pushover), the possibility of keeping the plastic hinge away from the location of link-to-column connection by using the RBS connection, were researched in a dual system of special moment frame and special eccentrically braced frame. According to this research, the models with RBS, by earlier developing the hinge at the RBS region, can delay yielding occurrence of link at the column face (at least prior to achieving the moment at the location of maximum flange decrease of RBS region) to 1.1 times its expected plastic moment capacity.

Keywords: Connections, Link, Eccentrically braced frame, Reduced beam section, Ductility.

1. INTRODUCTION

Eccentrically braced frames (EBF) are one of seismic load resisting systems in which the waste of energy (inelastic action) is performed through ductile links. In some of the common types of braced frames, one end of the link is attached to a column, and in these kinds of systems the correct behavior of this link is crucial for a safe performance of the EBF. But most of the tests implemented on these types of

* m-naghi@nit.ac.ir
† naghmeh.javadi@yahoo.com

doi:10.1016/j.proeng.2011.07.094

connection (before the Northridge earthquake (Engelhard et al, 1992) and after that (Tsai et al, 2000; Ricle et al, 2001; Okazaki et al, 2006)) show that most of the connections experienced sudden failures before achieving the required ductility. These failures were due to the intensity of stress imposed on the link-column connections. According to these tests improvements made in welding practices and other details in the connection did not suffice for better performance in these connections. The RBS connection, also known as the dog bone connection, was first used in moment frames. In these connections, reducing a portion of the beam flange at a short distance from the column (which results in moment stress concentration in this area) could result to a less amount of moment on the column and a less need for welding in the connection, and therefore, would result to a minimum fracture occurrence in these vulnerable areas (Engelhard et al, 1999). Among the available cutout types for these types of connection, the constant and tapered cuts have the tendency of stress concentration and flange-fracture in the RBS areas (Engelhard et al, 1999). In order to minimize the amount of tension concentration, Engelhard and his colleagues observed a radius cut in the connection which has shown positive performance and has lead to a common use of this type of cutout on the flanges in RBS areas (Engelhard et al, 1999). Engelhard and his colleagues proposed that the design of RBS connections should be in a way that the main purpose of its placement on the beam (which is to restrict the beam's moment) should be established on the face of the column. In designing the RBS connections, the main dimensions of the RBS (which are a=distance between the column face and the start of the RBS cutout, b=the length of the RBS area, and c=maximum RBS flange cutout) should be chosen in a way that the probable maximum moment at column face (M_f) would not exceed the beam's actual expected plastic moment (M_{exp}) when RBS reaches the hardening strain of 1.1 of its expected plastic moment (M_{eRBS}) under combined lateral earthquake and gravity loads. However according to the experiments the maximum hardening strain of the RBS could reach 1.15 times its expected moment capacity in this area (Engelhard et al 1999), but in design, 1.1 is used. It should be noted that the "a, b, c" parameters should be chosen within the practical domain which is obtained through experiments.

Therefore, it seems that RBS connections could be effective in changing the plastic hinge location and furthering it from the vulnerable area which is the face of the fuse beam. However considering the sharp slope of the moment diagram in the fuse beams compared to moment frames, the effectiveness of RBS section should be investigated. In this paper, a primary method for the use of RBS in the Fuse beam has been proposed and as a result the plastic hinge was moved away from the face of column. Also the ductility of the EBF frames with RBS connection and weight reduction of the structure was investigated for economic evaluation of the specimens.

2. THE OBSERVED MODELS

In order to observe the use of RBS in fractural fuse beams, a frame has been chosen from a three dimensional symmetric steel structure, which used dual special moment frame systems with EBF (D-shape) in both directions. The models were 2 series of 4, 7 and 10 story buildings, one with RBS and another without RBS, and were observed using the ETABS software for comparison. The models were loaded according to the Iranian loading codes of practice, and triangular earthquake loads were applied. The design of the frames was implemented according to allowable stress potion of AISC codes of practice, also models using RBS were designed according to the bending plastic capacity of RBS sections (figure 1).

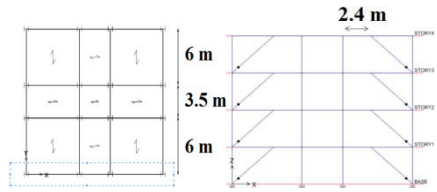

Figure 1: Plan and the chosen axis for modeling

3. THE PROPOSED METHOD FOR USING RBS IN FUSE BEAMS

According to the RBS design philosophy, and considering that the end moment of fuse beam (which is situated far from the face of the column) is less or equal to the moment at the face of the column. The following design procedure and diagram (figure 2) is proposed for using RBS in fuse beams. According to this procedure, at the maximum reduced area of the flange, when RBS hardening capacity reaches 1.1 of its expected plastic moment capacity at that area (M_{eRBS}), the end moment of the fuse beam at the face of the column (M_f) should not exceed the section expected moment capacity (M_{exp}).

$$M_f \leq M_{exp} \tag{1}$$

$$M_f = M_{eRBS} \times 1.1 + V_{RBS} S_h + w\frac{s_h^2}{2} \tag{2}$$

$$M_{exp} = Z_b F_y R_y \tag{3}$$

$$V_{RBS} = \frac{(M_{exp} + M_{eRBS} \times 1.1)}{e - s_h} + \frac{w(e - s_h)}{2} \tag{4}$$

$$M_{exp} = Z_b F_y R_y \tag{5}$$

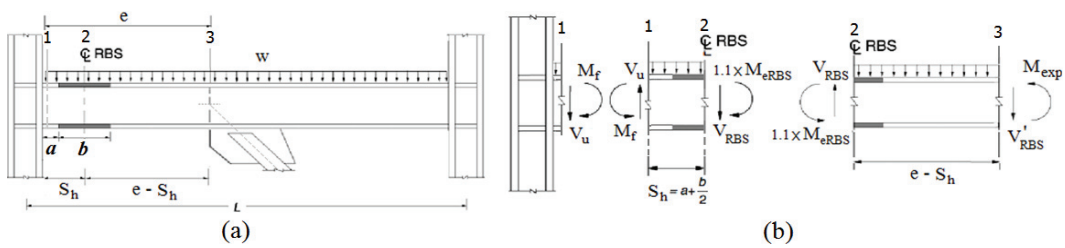

Figure 2: EBF beam; (a) RBS location in link; (b) free body diagram

In the mentioned equations, V_{RBS} is the total shear force at the maximum reduced section of RBS. w is uniform gravity load on the braced beam span. e is the length of the fuse beam. S_h is the distance between the maximum reduced RBS to face of the column. Z_b the plastic module of the beam and R_y is the ratio of the expected yield stress to the yield stress of the steel (F_y).

Considering the sharp slope of the of the moment diagram at the short length of the fuse beam, and also considering the practical domains in left parts of equations (6) to (8) of the fuse beam, which are

commonly used in designing RBS in moment frames, the following RBS parameters were considered as shown in right parts of equations 6 to 8.

$$a \approx (0.5b_f \text{ to } 0.75b_f) = 0.51b_f \tag{6}$$

$$b \approx (0.65d \text{ to } 0.85d) = 0.66d \tag{7}$$

$$c \approx (0.1b_f \text{ to } 0.25b_f) = 0.2b_f \tag{8}$$

In the mentioned equations, b_f is the width of the flange and d is the depth of the beam. According to the proposed method, the use of RBS would be possible only for certain sections and lengths of fuse beams. For example, in a 2 meters long fuse beam, subjected to 1.91 ton/m gravity loading, and with the key parameters selected according to equations 8 to 10, RBS could only be specifically be used for sections up to IPE 400, and sections equal and more that IPE 450, the equation 1 would not be satisfied.

4. MODELING IN ETABS

Since it is not possible to model a radius-cut of RBS in ETABS, it was replaced with an equivalent beam, which has the same stiffness. In Figs. 3(a) and 3(b) the symbols for original and equivalent RBS are presented, respectively. In the equivalent RBS according to Fig. 3(b), the width of the RBS in the middle, is equal to the minimum width of the original RBS, in order to control the stress ratio and nonlinear performance of the RBS in this region. The parameters a' and c' are unknown, and in order to have a positive value for c', a' was considered 0.45b. c' was achieved from equality of the two stiffness.

Based on Castiglione deformation's theorem and the offered model of FEMA 274 (see Fig. 4) the elastic stiffness of the link (K) with the length of e is the combination of shear (K_s) and flexural stiffness (K_m) as shown in Eqn. 9 and these stiffness's are computable by using Eqn. 10 and Eqn. 11, respectively. In below equations E, G, I and A_w are respectively elastic modulus, shear modulus, moment of inertia and web area of link at the x distance from the column face.

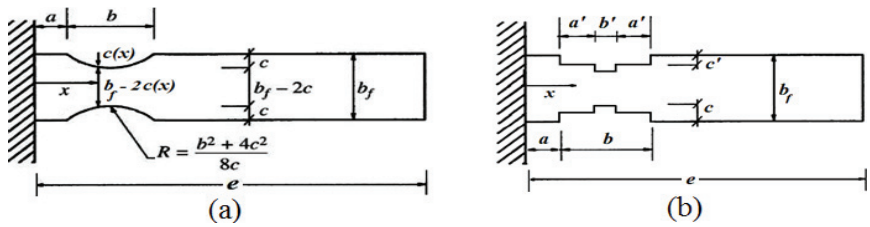

Figure 3: Link with RBS: (a) radius cut; (b) equivalent cut

$$1 = K\left(\frac{1}{K_s} + \frac{1}{K_m}\right) \Rightarrow K = \frac{K_s K_m}{K_s + K_m} \tag{9}$$

$$\frac{1}{K_s} = \frac{e}{GA_w} \tag{10}$$

$$\frac{1}{K_m} = \int_0^e \frac{(\frac{e}{2} - x)^2}{EI}\, dx \tag{11}$$

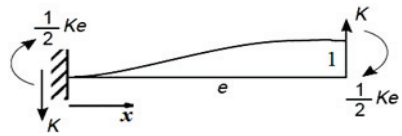

Figure 4: Offered model for computing elastic stiffness of link (FEMA 274)

According to Eq. 10, the shear stiffness's of the link in the two cases of Fig. 3 are equal, so the presence of RBS will have no effect on the shear stiffness. For obtaining flexural stiffness of link with original RBS cut (K_{mRBS}), inertia moment of section over RBS region, I(x), was formulated according to Eq. 12, by placing Eq. 13 (the cut depth of flange c(x)) in to it (The Taylor series has been used for simplifying). In the following equations a, b and c are key parameters of RBS design, R is radius of RBS cut (see Fig. 3(a)), I_0 , t_f and d are also moment of inertia for full link cross-section, flange thickness and depth of link.

$$I(x) = I_0 - \left[4c(x)t_f\left(\frac{d-t_f}{2}\right)^2 + 4c(x)\frac{t_f^3}{12}\right] \approx \frac{N_1}{2R}\left[\left(x-(a+\frac{b}{2})\right)^2 + N_2\right]$$

$$\dots(a \le x \le a+b) \tag{12}$$

$$c(x) = R\sqrt{1-\left(\frac{x-(a+\frac{b}{2})}{R}\right)^2} + c - R \approx R\left[1-0.5\left(\frac{x-(a+\frac{b}{2})}{R}\right)^2\right] + c - R = c$$

$$-0.5\frac{\left(x-(a+\frac{b}{2})\right)^2}{R} \quad \dots(a \le x \le a+b) \tag{13}$$

$$N_1 = t_f(d-t_f)^2 + \frac{t_f^3}{3} \tag{14}$$

$$N_2 = \frac{2R(I_0 - cN_1)}{N_1} \tag{15}$$

Based on Eqn. 11, the flexural stiffness of link with original RBS cut (K_{mRBS}) and also link with equivalent RBS cut (K'_{mRBS}) were obtained from Eqn. 16 and Eq. 17 which in Eq. 17, I_c and $I_{c'}$ (Eq. 18) are respectively inertia moment of the equivalent RBS in the sections with the cut depth of c and c'.

$$\frac{1}{K_{mRBS}} = \int_0^e \frac{(\frac{e}{2}-x)^2}{EI}dx = \frac{e^3}{12EI_0}\left[1 + \frac{12EI_0}{e^3}\left(\frac{1}{E}\int_a^{a+b}\frac{(\frac{e}{2}-x)^2}{I(x)}dx - \frac{(x-\frac{e}{2})^3}{3EI_0}\Big|_a^{a+b}\right)\right]$$

$$= \frac{e^3}{12EI_0}\left[1 + \frac{12EI_0}{e^3}\left(\frac{2R}{EN_1}\left(x + (a+\frac{b}{2}-\frac{e}{2})ln\left|(x-(a+\frac{b}{2}))^2 + N_2\right| + (\frac{e^2}{4}\right.\right.\right.$$

$$\left.\left.\left. + (a+\frac{b}{2})^2 - N_2 - (a+\frac{b}{2})e\right)\frac{1}{\sqrt{N_2}}tan^{-1}\left(\frac{x-(a+\frac{b}{2})}{\sqrt{N_2}}\right)\right) - \frac{(x-\frac{e}{2})^3}{3EI_0}\right)\Big|_a^{a+b}\right] \tag{16}$$

$$\frac{1}{K'_{mRBS}} = \int_0^e \frac{(\frac{Q}{2}-x)^2}{EI}dx = \frac{1}{3E}\left[\frac{1}{I_{c'}}\overbrace{\left((x-e/2)^3\Big|_a^{a+a'} + (x-e/2)^3\Big|_{a+b-a'}^{a+b}\right)}^{Q}\right.$$

$$\left. + \frac{1}{I_0}\overbrace{\left((x-e/2)^3\Big|_0^a + (x-e/2)^3\Big|_{a+b}^{e} + \frac{I_0}{I_0}(x-e/2)^3\Big|_{a+a'}^{a+a'+b'}\right)}^{Y}\right] = \frac{1}{3E}\left(Y + \frac{Q}{I_{c'}}\right) \quad (17)$$

$$I_{c'} - I_0 - N_1 c' \quad (18)$$

Finally through equating stiffness's, c' was obtained in accordance with Eqn. 19.

$$K'_{mRBS} = K_{mRBS} \Rightarrow c' = \frac{1}{N_1}\left(I_0 - \frac{Q}{\frac{3E}{K_{mRBS}} - Y}\right) \quad (19)$$

In this research, in order to investigate nonlinear performance of the frames, nonlinear static analysis (pushover), ETABS was used. Also the plastic hinges behavior were defined based on tables 5-6 and 5-7 of FEMA 356. The maximum linear expected strength (Q_{CE}) and the deformation at yield (θ_y) of moment hinges of links were also manually calculated and assigned based on Eqns. 20 and 21. In Eqn. 21 Z is the plastic modulus of section which hinge had been assigned to it.

$$\theta_y - \frac{2Q_{CE}}{K \times e^2} \quad (20)$$

$$Q_{CE} = M_{CE} = Z \times F_y \times R_y \quad (21)$$

5. RESPONSE MODIFICATION AND DUCTILITY FACTORS

In order to compare the ductility of models with and without RBS, the models response modification factors in accordance with Freeman method with several iterations were determined. In this method by determining the performance point through "capacity spectrum" method (ATC 40) and by using of Iranian normalize reflection spectra (National Building Code: part 6) the amount of R by was obtained according to two factors of capacity (R_C) and demand (R_D). In order to consider the effect of loading velocity (Uang 1991), the amount of R was computed by affecting 1.1 factor according to Eqn. 22. The ductility factors were also specified in accordance with Eqn. 23 by idealizing the “base shear-roof displacement curve” (capacity curve) to the bilinear curve, based on FEMA 356 where δ_m is the maximum displacement corresponding to performance point and δ_y is the displacement at yield point.

$$R = R_D \times R_C \times 1.1 \quad (22)$$

$$\mu = \frac{\delta_m}{\delta_y} \quad (23)$$

6. EVALUATION OF MODELS

6.1. Process of hinge formation

In Figs. 5(a) and 5(b) hinge formation process of models with and without RBS up to the failure point is illustrated by numbering. As shown in these figures, the first hinges of all models in accordance with anticipation were developed in the links. But this yielding in models with RBS has begun from the RBS region and the yielding of the column face has occurred with some delay. Whereas in models without RBS, the first hinge of links occurred at the critical region of the column face from the beginning.

6.2. Integrity investigation of RBS segment design

In order to see that the RBS presentation can delay the yielding occurrence of the column face, before RBS experiences 1.1 times its expected plastic moment (as mentioned in section 3), the locations of performance levels of "Life Safety (LS)" and "Collapse Prevention (CP)" were transferred to the locations which were corresponding to 1.1 and 1.15 times of the expected moment capacity of section, respectively. It is clear these alterations do not have any effect on the nonlinear analysis process and only displace the locations of performance levels on the behavior graph of the hinge.

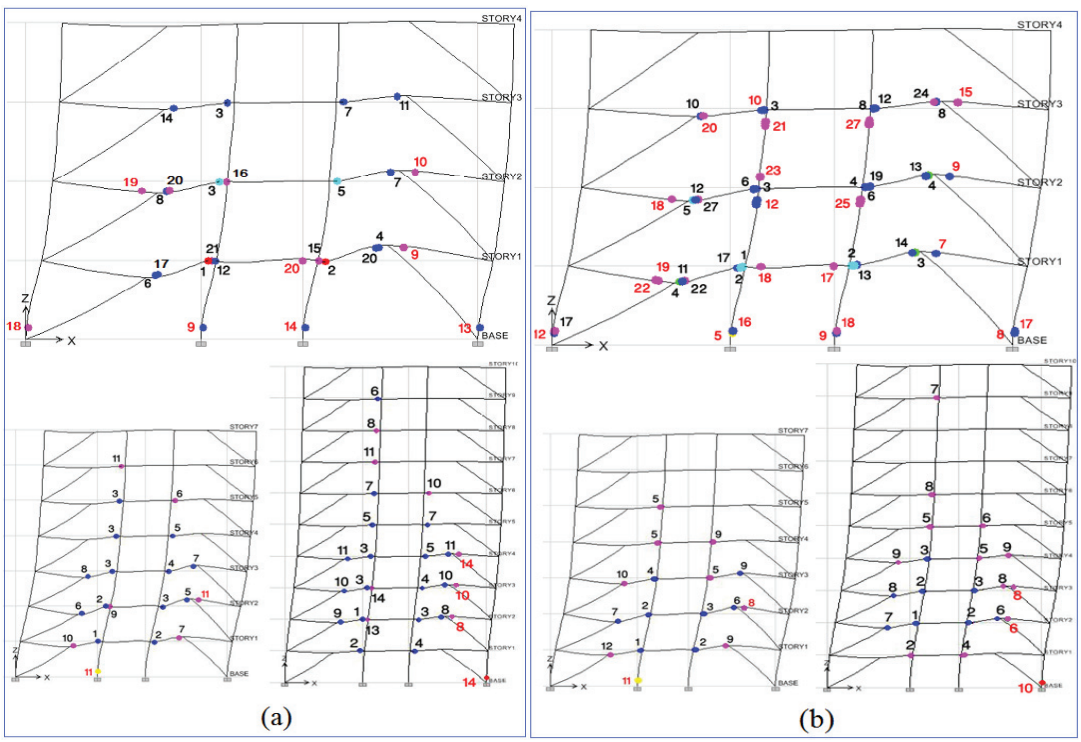

Figure 5: The process of the plastic hinge formation; (a) frames with RBS; (b) frames without RBS

According to this investigation as shown in Fig. 6, at the roof displacement of 0.098 m, in the first floor of the 4 story model, the RBS regions hinges have turned in to light blue (LS limit) and green (CP limit) colors, which means that they have passed the LS limit at 1.1 times of the expected moment

capacity, but the yielding has yet not occurred at the column face. At the roof displacement of 0.124 m (see Fig. 6), the RBS region hinge in the second floor has also experienced 1.1 times the expected moment, but at the column face has not formed any hinge yet. The process is the same for the second floor of the seven story model, and second and third model of the ten story model, as shown in figure 6.

6.3. Influence of RBS on the weight of models

The existence of RBS in the links, firstly reduces the imposed demands on the braces and columns by reducing the moment capacity of section and consequently reducing the shear strength of this type of links (considering the design of EBFs is based on the links capacity), and on the other hand can increase of dimensions of the structure members by reducing stiffness and increasing story's drift. In order to evaluate the influence of RBS on the models weight, a comparison between the weight of models with and without RBS were done with equal base shear design. The Fig. 7(a) shows the weight difference between these models versus the number of stories. As seen in this figure, in the 4 story models in which the drift category has a lower effect on the design process than other models, the RBS existence causes reduction of 39 kg of the weight of model with RBS. But by increasing the story numbers and appearance of the effects of drift, the weight of models with RBS has increased, instead of models without RBS. Although in spite the heavy weight of the models, the percentage of this increase as shown in Fig. 7(b) was not very much and does not exceed 0.1 percent.

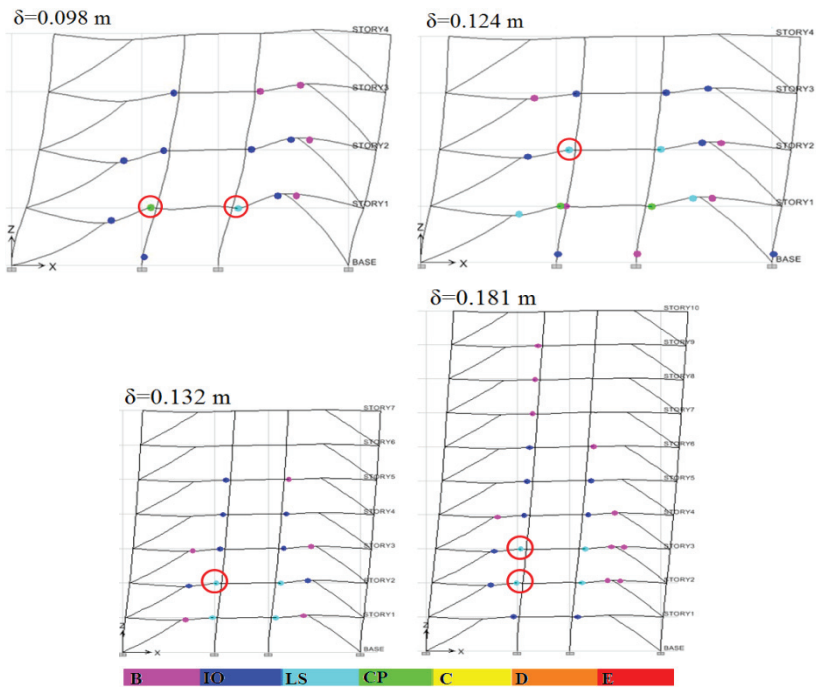

Figure 6: The hinge situation of RBS region prior to yielding the column at illustrated roof displacements

6.4. Ductility of models

The Figs. 8(a) and 8(b) illustrate the amount of the response modification and ductility factors obtained for models with and without RBS versus the number of stories. Scheming through these figures show that the amount of ductility and response modification factors of all the models with RBS have been increased compared to the models without RBS. The average value of this increase, in the ductility factor is 10.37% and in the response modification factor is 27.77%, which can be the cause of earlier formation of hinge at the RBS region.

7. SUMMARY AND CONCLUSIONS

In this paper the possibility of RBS existence in the long links or flexural links and its role on keeping the plastic hinge away from the link-to-column connection were investigated in three height levels of 4, 7 and 10 story buildings. According to this research, the existence of RBS in the link, in accordance with the offered design, can delay yielding occurrence of the link (at least before reaching the moment at the central location of RBS at the column's face) to 1.1 times its expected plastic capacity and also increase the ductility of system on the average, 10.37% in the ductility factor and 27.77% in the response modification factor. Furthermore, increasing the story numbers causes little weight increase of the models with RBS compared to the models without RBS. Finally, considering the offered design for RBS existence in the link, in this paper, this connection was merely recommended for very long links and also for the sections of links which are not very big. Therefore this type of connection cannot be utilized for all types of flexural links.

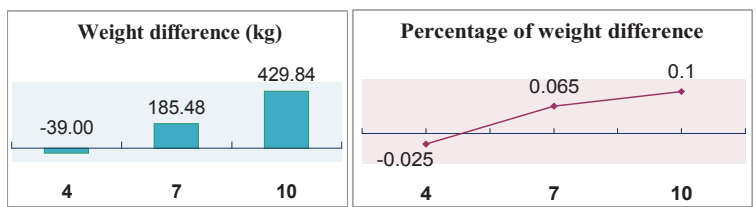

Figure 7: Comparison weight of models with and without RBS versus number of stories

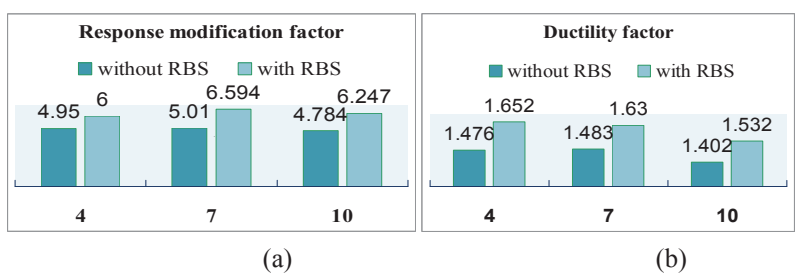

Figure 8: Comparison ductility of models with and without RBS versus number of story

REFERENCES

[1] Engelhard MD and Popov EP (1992). Experimental performance of long links in eccentrically braced frames. Journal of Structural Engineering. 118(11). pp. 3067–3088.

[2] Tsai KC, Engelhard MD and Nakashima M (2000). Cyclic performance of link-to-box column connections in steel eccentrically braced frames. Proceedings first International Conference on Structural Stability and Dynamics, Taipei, Taiwan, pp. 599-604.

[3] Ricles JM, Mao C, Lu L-W and Fisher JW (2001). Effect of local details on ductility of welded moment connections. Journal of Structural Engineering. 127(9). pp. 1036–1044.

[4] Okazaki T, Engelhard MD, Nakashima M and Suita M (2006). Experimental Performance of Link-to-Column Connections in Eccentrically Braced Frames. Journal of Structural Engineering. 132(8). pp. 1201–1211.

[5] Moore KS, Mally JO and Engelhard MD (1999). Design of Reduced Beam Section (RBS) Moment Frame Connections. Steel TIPS, Structural Steel Educational Council.

[6] ANSI/AISC 358 (2005). Prequalified Connections for Special and Intermediate Steel Moment Frames for Seismic Applications. American Institute of Steel Construction, Chicago.

[7] ETABS Version 9.2 (2008). Computers and Structures. Inc., Berkeley, California, USA.

[8] Ministry of Housing and Urban Development (2006). Iranian National Building Code: part 6 (Loads). Third Edition.

[9] ANSI/AISC 341 (2005). Seismic Provisions for Structural Steel Buildings. Supplement No. 1.

[10] ANSI/AISC 360 (2005). Specification for Structural Steel Buildings.

[11] FEMA 274 (1997). NEHRP Commentary Guidelines for The Seismic Rehabilitation of Buildings. Federal Emergency Management Agency, SAC Joint Venture.

[12] FEMA 356 (2000). Prestandard and Commentary for The Seismic Rehabilitation of Buildings. Federal Emergency Management Agency, SAC Joint Venture.

[13] Freeman SA (1992). On The Correlation of Code Forces to Earthquake Demands. Proceedings fourth U.S. Japan Workshop on the Improvement of Building Structural Design and Construction Practices.

[14] ATC 40 (1996). Seismic Evaluation and Retrofit of Concrete Buildings. Vol. 1, Applied Technology Council, California.

[15] Uang CM (1991). Establishing R (or RW) and Cd Factors for Building Seismic Provisions. Journal of Structural Engineering. 117(1). pp. 19–28.